ELSEVIER
SAUNDERS

Cardiol Clin 25 (2007) 15–33

CARDIOLOGY
CLINICS

Assessment of Ventricular Function with Cardiovascular Magnetic Resonance

Thomas F. Walsh, MD[a], W. Gregory Hundley, MD, FACC, FAHA[a,b,*]

[a]*Department of Internal Medicine, Wake Forest University School of Medicine, Bowman Gray Campus, Medical Center Boulevard, Winston-Salem, NC 27157-1045, USA*
[b]*Department of Radiology, Wake Forest University School of Medicine, Bowman Gray Campus, Medical Center Boulevard, Winston-Salem, NC 27157-1045, USA*

Management of patients who have cardiovascular disorders depends on assessments of global and regional left ventricular (LV) and right ventricular (RV) function. The high spatial and temporal resolution of cardiovascular magnetic resonance (CMR) images makes it well-suited for use in the assessment of RV and LV function. This article reviews CMR methods used to assess regional and global ventricular function.

Image acquisition techniques

Gradient echo

Gradient echo, also known as fast low-angle shot or FLASH [1] imaging, is the most extensively studied technique for assessing ventricular wall motion, volumes, and ejection fraction [2]. With gradient-echo imaging, the movement of the blood pool provides bright contrast against the gray appearance of the myocardium [3]. Previous studies have demonstrated the utility of gradient-echo imaging in the assessment of RV and LV volumes, mass, and ejection fraction [4–10].

True fast imaging with steady-state free precession

Fast imaging with steady-state precession refocuses the signal between excitations resulting in heightened blood pool—myocardial tissue contrast [11]. This technique can be used to acquire cine images with short repetition (<3 milliseconds) and echo (<1.5 milliseconds) times [12–16]. As can be seen in Fig. 1, the contrast between the LV endocardial surface and blood pool appears high even when LV systolic function is reduced [17].

Echo planar imaging

Gradient echo planar imaging (EPI) sequences acquire single snapshots of LV wall motion during 40- to 60-millisecond intervals. By placing these acquisitions in series, LV wall motion can be visualized in near real time. Importantly, chemical shift artifacts, and the relatively long temporal resolution of current techniques (60 milliseconds) inhibit identification of end systole for determination of ejection fraction and LV end systolic volume when heart rates are high [18].

Sensitivity-encoding scheme

With the sensitivity-encoding scheme (SENSE), the resonance signal is encoded by spatially varying the receiver sensitivity of the phased array elements [19]. Using simultaneous signal acquisition with multiple parallel receiver coils, the speed of data collection is not limited by sequential data from gradient encoding acquisitions. For this reason, scan times can be reduced by a factor related to the number of coils in the array [20,21]. In one study

Dr. Hundley is supported in part by National Institutes of Health R21CA109224, and R21/R33CA121296, and an industrial grant from Bracco Diagnostics.

* Corresponding author. Department of Internal Medicine (Cardiology Section), Wake Forest University School of Medicine, Bowman Gray Campus, Medical Center Boulevard, Winston-Salem, NC 27157-1045.
E-mail address: ghundley@wfubmc.edu (W.G. Hundley).

0733-8651/07/$ - see front matter
doi:10.1016/j.ccl.2007.01.002

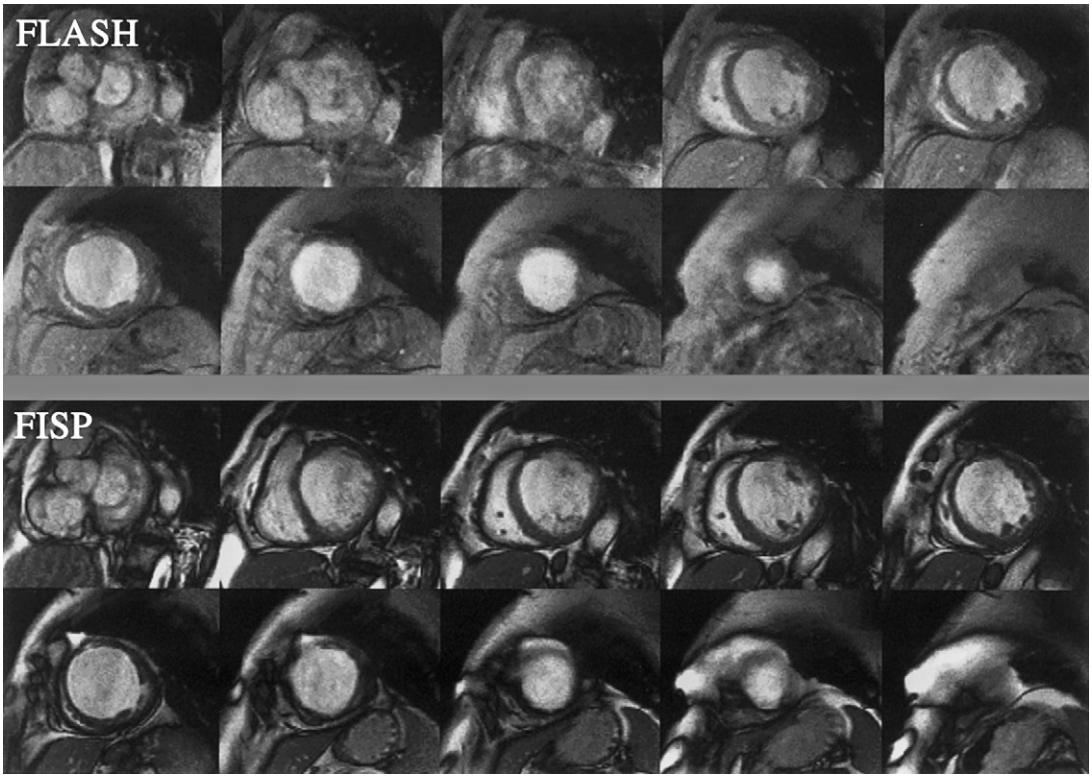

Fig. 1. Gradient echo and steady-state free precession. Images from a patient who presented to an emergency room with chest pain. The top panel is a gradient echo also known as a fast low-angle shot (FLASH) image. The bottom panel illustrates the superior image quality of SSFP. (*From* Moon JC, Lorenz CH, Francis JM, et al. Breath-hold FLASH and fast imaging with steady-state precession cardiovascular imaging: left ventricular volume differences and reproducibility. Radiology 2002;223:789–97; with permission.)

by Pruessmann and colleagues [22], a temporal resolution of 13 milliseconds was acquired with three parallel slices. This technique may lead to further improvements in providing real-time images of cardiovascular function.

Tissue tagging

With myocardial tissue tagging, radiofrequency pulses are used to create regular dark banks of selective saturation before initiation of the remainder of the imaging sequence. Consequently, motion of material can be tracked as the saturation bands deform [4]. Using this technique, termed spatial modulation magnetization (SPAMM), myocardial contraction or relaxation can be quantified. Tagging bands usually disappear after 400 to 500 milliseconds. Therefore a tagging grid can be obtained, followed by a saturation pulse (termed: complimentary spatial modulation magnetization [CSPAMM]) to create a negative grid in the second or diastolic portion of the imaging acquisition (Fig. 2) [23–25].

Displacement encoding with simulated echos

Recently, a new technique termed displacement encoding with simulated echoes (DENSE) has been described that allows one to track myocardial motion data using phase-reconstructed images. Similar to tagging, DENSE uses spatial modulation of magnetization to position encode magnetization at a point in time and follow tissue displacement during a subsequent portion of the cardiac cycle [26,27]. Compared with CSPAMM, DENSE allows one to differentiate LV regional function within the endocardium, midmyocardium, and epicardium (Fig. 3).

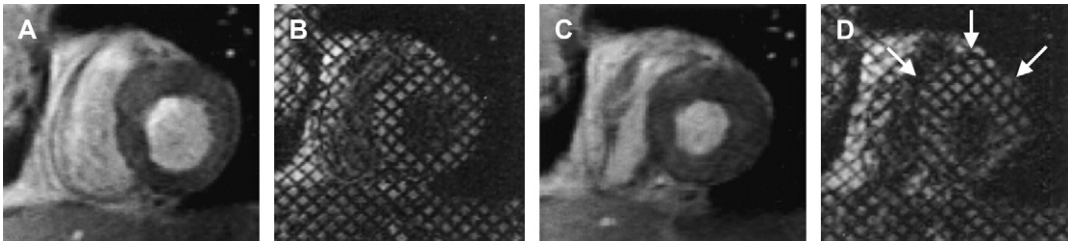

Fig. 2. Tagging of the left ventricle. Images of a patient without (*A*) and with (*B*) tagging during the diastolic phase of a normal left ventricle at rest. (*C, D*) are comparative images at peak stress. There is akinesea of the anterior, anterior–septal, and septal walls indicating ischemia. (*From* Wahl A, Paetsch I, Roethemeyer S, et al. High-dose dobutamine–atropine stress cardiovascular MR imaging after coronary revascularization in patients with wall motion abnormalities at rest. Radiology 2004;233:210–6; with permission.)

Phase contrast MRI

Measurement of motion with MRI also can be done through velocity phase mapping [28–32]. With this method, the change in phase of the net magnetization inside each pixel is related to the velocity of the tissue in the direction parallel to the magnetic field. With this technique, the entire cardiac cycle can be evaluated without an elaborate pulse sequence, as it is insensitive to T1 relaxation [33–38]. To date, this technique has received limited use because of lengthy scan times and time-consuming analyses of the acquired image data.

Rest measures of right and left ventricular volume and ejection fraction

Left ventricular volume and ejection fraction

There are several different methods available for measuring left ventricular volume and ejection fraction with CMR. The two most common include the Simpson's rule technique and area-length technique. With the Simpson's rule technique, LV volumes are determined by summing the endocardial area within multiple short axial slices spanning the base to the apex of the heart and multiplying each area determination by slice thickness (Fig. 4) [5,39,40]. This technique is

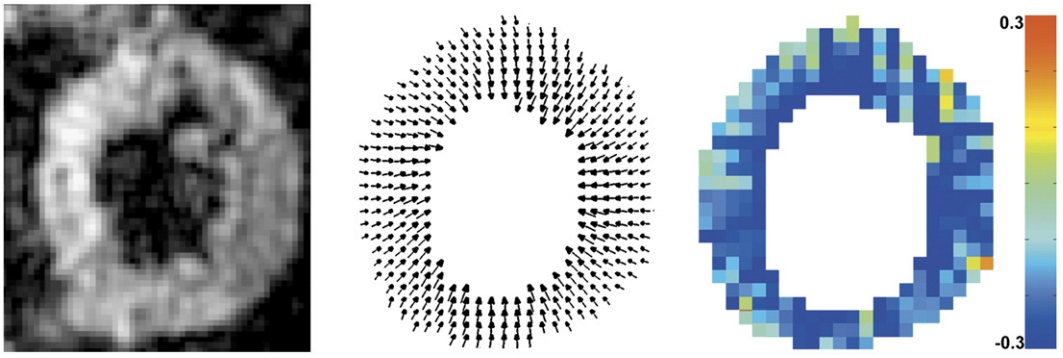

Fig. 3. Short axis displacement encoding with simulated echoes images of the left ventricle. These figures were obtained in single breath hold in a healthy volunteer. The far left figure is of a magnitude reconstruction of the short axis view of the left ventricle. The middle figure is a two-dimensional displacement map computed from a phase-reconstructed image with each vector in the map representing the end–diastolic to end–systolic motion of the myocardium as depicted in a single pixel. The far right figure demonstrates circumferential shortening as computed from the displacement field as a color-coded myocardial strain map. (*From* Kim D, Gilson WD, Kramer CM, et al. Myocardial tissue tracking with two-dimensional cine displacement-encoded MR imaging: development and initial evaluation. Radiology 2004:230:862–71; with permission.)

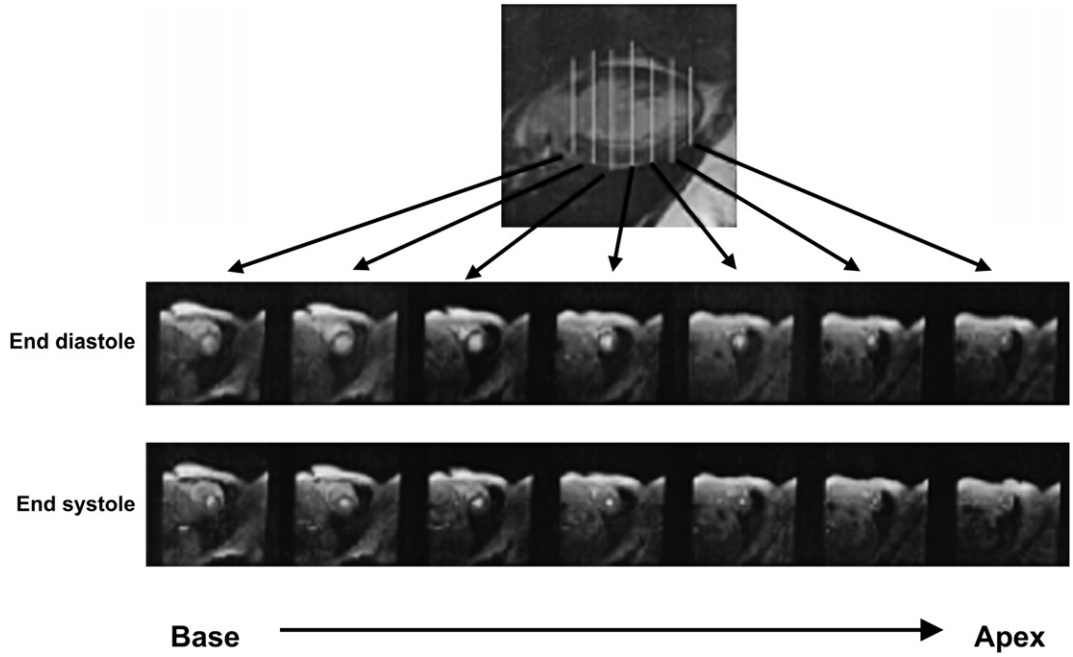

Fig. 4. Gradient echo images of sequential multiple slices of the left ventricle in short-axis planes (from base to apex) are displayed for determining left ventricle volume by Simpson's rule. Endocardial area in each segment is measured at end diastole (top row) and end–systole (bottom row). Left ventricular volume is calculated by the summing the endocardial area within each slice and multiplying by the slice thickness. Left ventricular ejection fraction equals (end–diastolic volume−end–systolic volume)/end–diastolic volume.

advantageous, because one can calculate LV volumes without using formulae that require assumptions about LV shape. For this reason, the Simpson's rule technique is useful in patients who have cardiomyopathy or regional wall motion abnormalities.

The area length techniques are based on formulae that assume the left ventricle exhibits the shape of a prolate ellipse. With the single-plane or biplane area-length methods, only one or two slice acquisitions are required, and image analysis time is short [41,42]. Because patients who have distorted LV geometry caused by dilated cardiac chambers or resting regional wall motion abnormalities do not exhibit left ventricles in the shape of a prolate ellipse, LV volume determinations may be less precise than those generated with the Simpson's rule method [43]. With both methods, LV ejection fraction is calculated by subtracting end–diastolic volume from end–systolic volume and dividing by end–diastolic volume.

Assessments of LF volumes measured with the Simpson's rule technique have been validated with cadaver studies. In 1985, Rehr and colleagues [39] used cadaver hearts and created latex casts of excised human left ventricles to compare CMR measurements derived from scanning the casts with actual volume measurements from the casts themselves. They found excellent correlation between CMR-determined measurements and cast measurements ($r = 0.997$, standard error of the estimate equal to 4.3 to 4.9 mL over a range of 26 to 190 mL [Fig. 5]). Other studies have performed similar analyses from autopsy series and found excellent correlations also [5].

Data from animal models have confirmed the findings in phantom and cadaver studies. Keller and colleagues [44] examined canine hearts and found a close correlation ($r = 0.98$) between LV mass and volumes measured with CMR and those calculated by the volume of displacement method. In another study by Koch and colleagues [45], eight porcine hearts were explanted and prepared by removal of the atria. The correlation between measures obtained from both ventricles and the CMR-derived measures was greater than 0.99. Multiple studies have been performed in canine,

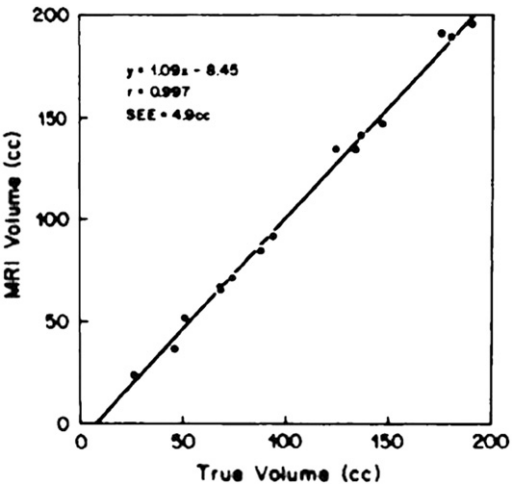

Fig. 5. Cardiovascular magnetic resonance of human casts. Relation between volume calculated using MRI and true volume (superimposed on regression line relating the two) for the images obtained using normal resolution. Regression line is calculated using all 15 casts. (*From* Rehr RB, Malloy CR, Filipchuk NG, et al. Left ventricular volumes measured by MR imaging. Radiology 1985;156:717–9; with permission.)

porcine, rat, and mice models to confirm excellent correlation between CMR-calculated ventricular volumes and actual volumes measured by timed volume collections [46–49].

Assessment of LV volumes and EF with CMR using cine gradient echo techniques in people in vivo with both normal and abnormal LF morphology is highly reproducible and exhibits low intraobserver and interobserver variability [50–53]. Ventricular volumes, mass, and ejection fraction also can be assessed with a high degree of accuracy in patients who have congestive heart failure. As small as a 5% difference in LV ejection fraction with 90% power and $\alpha = 0.05$ can be detected in subjects who have impaired LV function.

Because of the heightened reproducibility and low variance of this method, small sample sizes can be used when a change in LV volumes or EF by CMR serve as a study endpoint. In comparison with sample sizes required through the use of area-length methods acquired through other invasive and noninvasive imaging modalities, CMR measures have been demonstrated to be more precise and reproducible [54]. For this reason, studies using CMR measures of LV volumes and ejection fraction require sample sizes that are 80% to 90% smaller then the sample sizes needed with other modalities [54].

The white blood imaging technique used to assess LV volumes may influence the calculated measures derived from CMR. One study comparing short axis cine magnetic resonance (MR) images with steady-state free precession and gradient-echo techniques indicated that LV ejection fraction was lower and LV mass, end-systolic, and stroke volumes were higher in the steady-state free precession technique when compared with the measures from the gradient-echo sequences. The heightened contrast between the blood and myocardial border are thought to be the source of these discrepancies [55].

Right ventricular volume and ejection fraction

Because of the shape and location of the right ventricle beneath the sternum, quantification of RV volumes and ejection fraction is difficult with echocardiography or radionuclide ventriculography. With CMR, there are no limitations imposed by body habitus, and thus, as with LV functional measures, RV volumes and ejection fraction can be determined accurately [56–60]. In studies with normal volunteers, there has been low intraobserver, interobserver, and interstudy variability (5% to 6%) [61].

Two studies have reported normative CMR values for the right ventricle. Rominger and colleagues [60] reported an average RV end–diastolic volume index of 78 plus or minus 15 mL/m^2, an average end–systolic volume index of 30 plus or minus 9 mL/m^2, and an average ejection fraction of 62% plus or minus 6% in 52 healthy volunteers aged 18 to 58 years. Lorenz and colleagues [61] found similar results in 75 healthy participants ranging in age from 8 to 55 years. In this study, the RV end–diastolic volume index averaged 75 plus or minus 13 mL/m^2, and the RV ejection fraction averaged 61% plus or minus 7%.

Assessment of left ventricular regional function

Wall motion

CMR is an excellent technique for visualizing wall motion. Using various white blood imaging techniques, cine loops can be constructed during 3- to 4-second periods of breath holding. Because CMR can acquire images in virtually any tomographic plane, standard apical (long axis, four-chamber, and two-chamber) and short-axis (basal, middle, and apical) views of LV wall motion can

be obtained without limitation imposed by body habitus (Fig. 6).

Wall thickening

Two primary methods have been described for the assessment of LV wall thickening: the center line method and myocardial tissue tagging [62–64]. With the center line technique, a line is created in the center of the myocardium equidistant from the epicardial and endocardial borders. Perpendicular to the center line, multiple chords are evenly distributed circumferentially around the LV myocardium at specified intervals, with the length of each chord identifying local wall thickness (defined as the ratio of the length of the chord at end systole to end diastole) [37]. After myocardial infarction (MI), this technique has been used to identify abnormal thickening associated with the site and extent of the infarct [48,65]. This technique also has been used during dobutamine MR stress testing to identify abnormal thickening in association with myocardial ischemia. The sensitivity of detecting luminal narrowings of greater than 50% in one, two, and three epicardial arteries was 88%, 91%, and 100%, respectively [66]. A limitation of this technique is the fact that when the imaging slice is not positioned perpendicular to the long axis of the left ventricle, local wall thickness (and consequently,

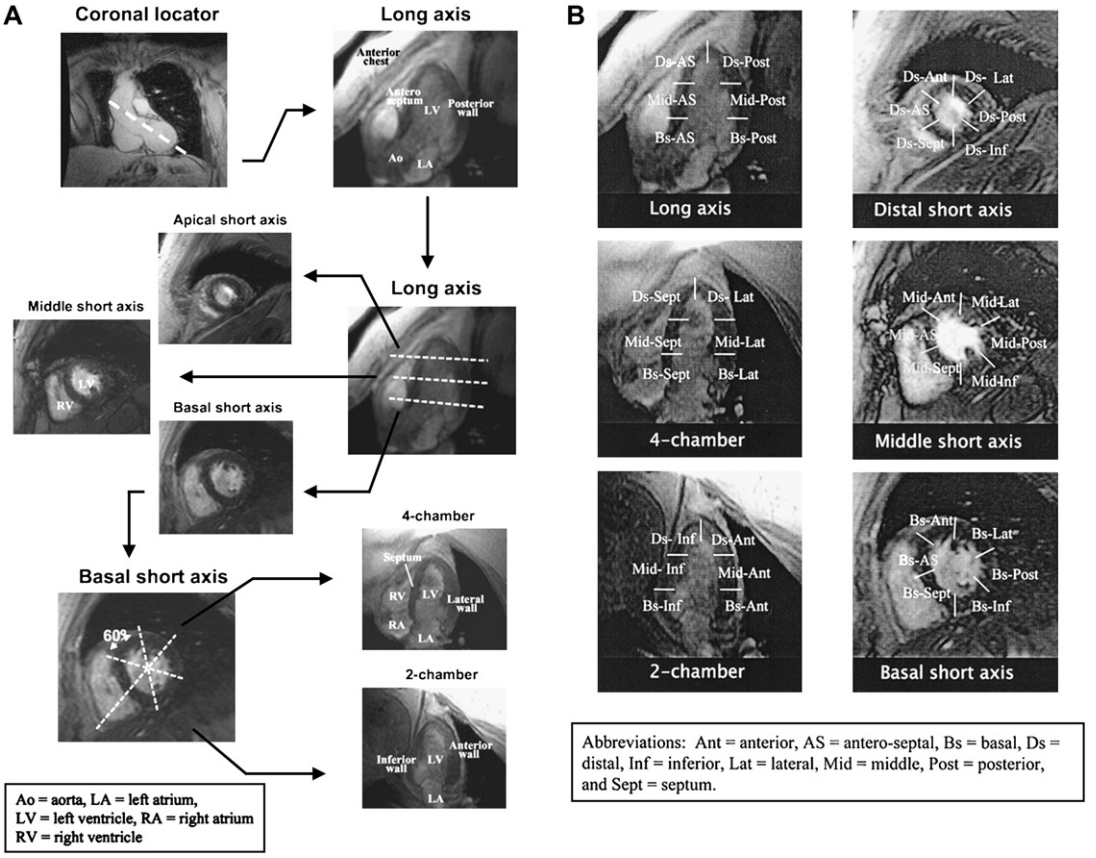

Fig. 6. Method for obtained standard views. (*A*) Illustration of a method for obtaining three short-axis (basal, middle, and apical) and three apical (long-axis, four-chamber, and two-chamber) cardiovascular magnetic resonance views of the left ventricle. In all images, the myocardium is gray, and the blood pool white. The white dotted lines on the coronal locator, long-axis view, and basal short-axis view indicate the slice positions for obtaining the subsequent views demarcated by the black arrows. (*B*) The 18 myocardial segments are demarcated by white lines. (*From* Hundley WG, Morgan TM, Neagle CM, et al. Magnetic resonance imaging determination of cardiac prognosis. Circulation 2002;106(18): 2328–33; with permission.)

wall thickening) may be overestimated. Additionally, through-plane myocardial motion is not accounted for as the heart translates from diastole to systole [66].

Tagging can be used to monitor wall thickening throughout the cardiac cycle. By tracking the side-to-side separation of tag lines or tag line intersections or the change in distance between line pairs, myocardial shortening or elongation can be observed [67]. With this approach, it is possible to measure wall thickness across the LV myocardium [67,68].

Left ventricular strain

Measurements of LV strain are useful in that they are not dependent on volume loading or preload in the determination of ventricular relaxation [69]. Strain analysis can be used to characterize regional deformation of the myocardium. Strain can be defined as the percent change in length per unit of initial length. Normal strains can be analyzed in radial (E_{rr}), longitudinal (E_{ll}), and circumferential (E_{cc}) axes. Shear strains are defined in the plane between two coordinate axes in which the strain between the circumferential and longitudinal axis is E_{cl}; the strain between the circumferential and radial axis is E_{cr}; and the strain between the longitudinal and radial axis is E_{lr} [67,70]. To date, strain has been assessed with both CSPAMM and DENSE techniques. Using sonomicrometric measurement techniques, measurements of myocardial thickening and strain by tagged MR imaging have been validated [71]. In a recent study examining LV diastolic dysfunction in patients who had type 2 diabetes mellitus and normal LV ejection fractions, it was found that peak LV systolic circumferential and longitudinal shortening values were lower in the patients who had diabetes compared with normal controls [72]. In hypertensive patients who have LV hypertrophy, it has been found that intramural myocardial strain is abnormal [73]. Investigators in other studies have used myocardial strain assessments and tissue tagging to evaluate patients who have myocardial ischemia, infarction, hibernating or stunned myocardium, or postinfarction remodeling (Fig. 7) [74,75].

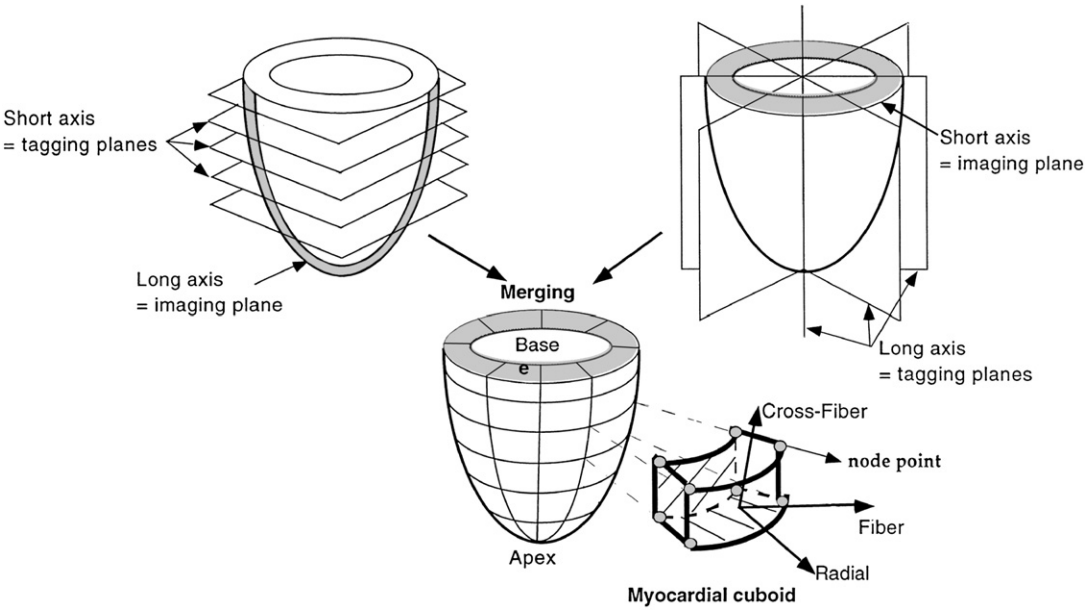

Fig. 7. Magnetic resonance (MR) tagging used for regional strain analysis. The left ventricle is divided into 32 small cuboids by means of a combination of MR tagging along five cardiac short- and four long-axis planes. Each cuboid is constructed from four subendocardial and four subepicardial node points. Strains are expressed in local cardiac coordinate system for each subepicardial and subendocardial node point. Axes are radial (R) using the direction perpendicular to wall; fiber (F), tangent to surface and parallel to local fiber direction at either epicardium or endocardium; and cross-fiber (X), tangent to surface and perpendicular to F. (*From* Bogaert J, Maes A, Van de Werf F, et al. Functional recovery of subepicardial myocardial tissue in transmural myocardial infarction after successful reperfusion: an important contribution to the improvement of regional and global left ventricular function. Circulation 1999;99(1):37; with permission.)

Regional relaxation

Relaxation is a highly ATP-dependent process, and thus if abnormalities of relaxation can be measured, they may be more sensitive markers of abnormal LV performance than measures reliant upon assessments of LV systole. Paetsch and colleagues [76] evaluated the diastolic parameters from myocardial tagging of 25 patients who had low- and high-dose dobutamine stress to identify patients with flow-limiting epicardial coronary arterial luminal narrowings. They showed that myocardial tagging helps in a quantitative analysis of systolic and diastolic function during low- and high-dose dobutamine stress. They concluded that the diastolic parameter of time to peak untwist assessed during low-dose dobutamine stress was the most promising global parameter for identification of patients who had flow-limiting epicardial coronary arterial luminal narrowings.

Assessment of right ventricular regional function

CMR has been used to assess RV function in patients who have congenital heart disease [77–79], pulmonary hypertension [80–82], and other disorders such as arrhythmogenic RV cardiomyopathy (ARVC) [83–85]. Keller and colleagues [86] studied 36 patients who had suspected ARVC. The diagnosis was confirmed by CMR in 16 of 18 patients who had a clinical diagnosis of ARVC (sensitivity 89%), and correctly excluded in 14 of 17 patients who had clinically excluded ARVC (specificity 82%). Importantly, in ARVC, CMR is suited well for assessing fatty infiltration of the RV free wall and the consequent regional wall motion abnormality associated with the fatty infiltration (Fig. 8).

Dynamic measures of left ventricular function

Detection of ischemia

Over the last decade, software and hardware advances have enabled investigators to demonstrate the clinical utility of CMR wall motion stress testing in patients referred for cardiovascular care. This has been accomplished using phased-array surface coils, fast scans with short repetition and echo times, advanced gating systems, specialized software for image display during stress testing, and intravenous administration and hemodynamic measurement (heart rate, oxygen saturation, blood pressure) equipment that allow for the safe monitoring of patients during the course of stress testing [87]. To date, in general, LV wall motion during CMR stress testing has been assessed across LV myocardial segments (as recommended by the American Heart Association) using a four-point scoring system (1 is normal; 2 is hypokinetic;3 is akinetic, and 4 is dyskinetic) similar to that used with dobutamine stress echo (DSE). A deterioration score of 1 or higher is used to identify ischemia.

The first clinical use of CMR for the detection of inducible ischemia was reported by Pennell and colleagues [88]. In this study, CMR was compared with thallium-201 single photon emission CT (PET) and coronary angiography. Twenty-five study subjects received dobutamine infusions of up to 20 μg/kg/min and underwent conventional gradient-echo cine CMR. Twenty-two participants had significant coronary artery disease (CAD) with angiography, and of these 20 had wall motion abnormalities as per CMR compared with 21 identified as having reversible ischemia by dobutamine thallium tomography. Consequently, the sensitivity of CMR for detection of significant CAD in this study was 91%. Between PET and CMR, there was a 96% agreement at rest, 90% agreement during stress, and 91% agreement for the assessment of reversible ischemia. This study was the first to demonstrate in patients who had CAD that CMR could be used effectively to assess LV regional function.

In another early study, Baer and colleagues [89]. This source is incorrect. Please see below compared stress dobutamine CMR results with those obtained using dipyridamole CMR testing in 61 patients who had a normal ejection fraction and known 70% stenoses of one of three epicardial coronary arteries. Thirty-three patients had wall motion assessed after high-dose dipyridamole infusion (0.75 mg/kg over 10 min), and 28 patients underwent wall motion assessments with dobutamine infusion (5, 10, 15, and 20 μg/kg/min). In basal and midventricular short-axis planes, segmental wall motion analysis was performed. The sensitivity of dipyridamole CMR and dobutamine CMR for detecting coronary artery luminal narrowing greater than 70% was 84% and 85%, respectively.

van Rugge and colleagues [90] used patients who had known wall motion abnormalities to assess the efficacy of quantitative measurements during dobutamine stress CMR for detection and localization of myocardial ischemia. Thirty-nine patients with prior wall motion abnormalities

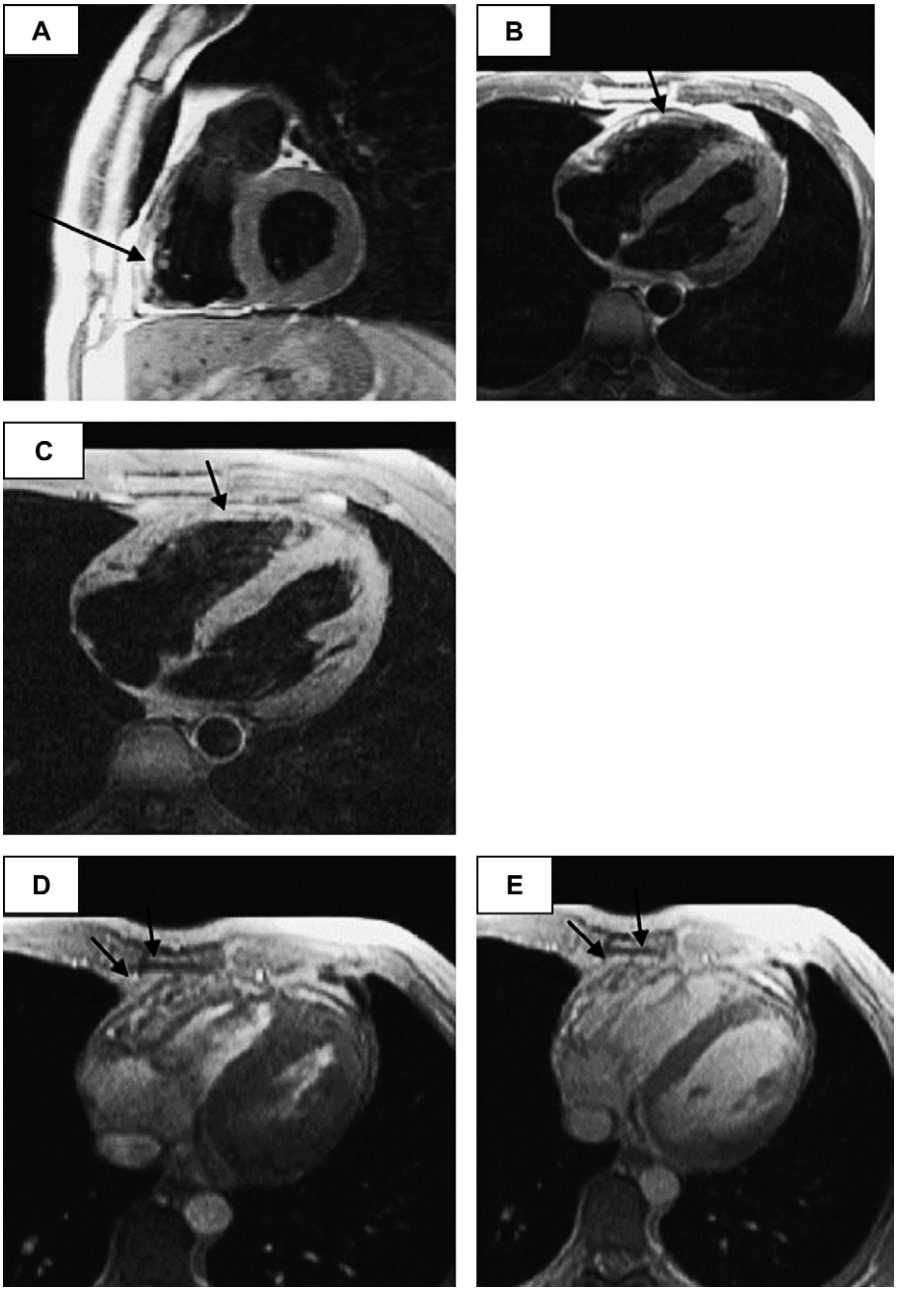

Fig. 8. Cardiovascular magnetic resonance imaging for the diagnosis of arrhythmogenic right ventricular dysplasia. T1-weighted turbo spin–echo sequences show the high signal intensity (bright) region within the right ventricular (RV) anterior wall in a left ventricular (LV) short-axis (*A*) and axial (*B*) view (arrows). Signal intensity of this region is comparable to that of subcutaneous fat. With application of a fat suppression pulse, the bright signal of the fatty infiltrates disappear, again comparable with subcutaneous fat (*C*) (arrow). End–systolic (*D*) and end–diastolic (*E*) frames from a cine gradient echo sequence demonstrate the RV dilation and the impaired inward motion and systolic thickening of the RV anterior wall (arrows). (*From* Keller D, Osswald S, Bremerich J, et al. Arrhythmogenic right ventricular dysplasia: diagnostic and prognostic value of cardiac MRI in relation to arrhythmia free survival. Int J Card Imaging 2003;19:537; with permission.)

and 10 without were assessed with gradient-echo dobutamine cardiovascular magnetic resonance at rest and during peak dobutamine stress (infusion rate of 20 μg/kg/min). They found excellent sensitivity (91%) and specificity (80%) for the detection of significant CAD (diameter stenosis $\geq$50%) with dobutamine stress CMR [91].

Each of these early studies demonstrated the diagnostic utility of stress CMR for detection of wall motion abnormalities in patients who had known disease. They were limited by wall motion analysis at baseline compared only with peak stress and not continuously throughout testing. As noted previously, these studies were relatively small (20 to 60 patients) and were performed in a single institution. In addition, infusions were terminated prematurely when patients developed chest pain. Nevertheless, this series of small studies highlighted the feasibility of dobutamine administration in the CMR environment and showed that diagnostic utility of these techniques may be high.

Two major studies were performed that demonstrated the feasibility of DCMR in patients with known or suspected CAD without awareness of the extent of coronary arteriosclerosis before testing. Nagel and colleagues [92] compared DSE with DCMR in 208 patients referred for contrast coronary angiography (cross-reference). CMR provided better sensitivity (89% versus 74%) and specificity (86% versus 70%) for detecting 50% or more cases of coronary arterial luminal narrowing with coronary angiography compared with DSE. In a second study, Hundley and colleagues [87] used DCMR to study patients who had poor acoustic windows that prevented the use of second harmonic DSE imaging. When compared with contrast coronary angiography, the sensitivity and specificity were 83% for detecting coronary arterial luminal narrowing of greater than 50% [93]. Assessment of myocardial perfusion and wall motion during DMR imaging appears to improve the diagnostic accuracy of MRI stress tests compared with wall motion analysis alone [94].

Subsequently, other investigators have substantiated the utility of CMR wall motion stress testing. Sensky and colleagues [95] examined the accuracy of CMR results when compared with angiography in identifying regions of ischemia in patients who had multivessel coronary arteriosclerosis before coronary artery revascularization. Using steady-state free precession sequences combined with parallel imaging acquisitions, Paetsch and colleagues [96] acquired images to identify at least 50% of coronary arterial luminal narrowings with a sensitivity and specificity of 89% and 80%, respectively. Zoghbi and colleagues [97] emphasized the high diagnostic accuracy, feasibility, versatility, and relatively low cost and high sensitivity (91%) and specificity (85%) for diagnosing CAD compared with DSE (with a sensitivity of 85%). In these studies, implementation of newer white blood imaging techniques reduced scan times by factors of three to four, allowing the acquisition of multiple slice positions during a single breath hold.

Although many earlier studies excluded patients who had a prior MI or wall motion abnormalities at rest, in 2004, Wahl and colleagues [98] evaluated a group of 160 patients to document the utility of DCMR in patients who had previously documented resting wall motion abnormalities. The subjects were difficult to assess with DSE because of the variability in interpreting wall motion with poor visualization. Additionally, they had prior revascularization with underlying resting LV wall motion abnormalities. The sensitivity and specificity of DCMR for detecting coronary luminal narrowing of at least 50% in this patient population was 89% and 84%, respectively. In addition, the sensitivity of detecting luminal narrowing of one, two, or three epicardial arteries was 87%, 91%, and 100%, respectively. This study demonstrated that high-dose DCMR can be useful even in patients with previously documented wall motion abnormalities and a history of coronary revascularization.

In 2003, Kuijpers and colleagues [99] reported on the qualitative assessment of tagged images in comparison with nontagged cine CMR. One hundred ninety-four patients referred for the evaluation of chest pain underwent tagged dobutamine stress wall motion analyses and contrast coronary angiography. Tagged DCMR images detected new wall motion abnormalities in 68 patients, compared with 58 patients without tagged images. This was the first study to demonstrate that high-dose DCMR with tagging may improve the utility of wall motion assessments alone for detecting inducible LV wall motion abnormalities indicative of ischemia during dobutamine CMR stress testing. As shown in Table 1, multiple studies have been performed that demonstrate the clinical utility of CMR wall motion stress testing in diagnosing more than 50% of epicardial coronary arterial luminal narrowings. Combing the results from all studies, the sensitivity and specificity of dobutamine stress CMR was 86% and 84%,

Table 1
Sensitivity and specificity analysis for stress dobutamine cardiovascular magnetic resonance in detection of ≥50% coronary arterial luminal narrowings

Author/year	Dose (μg/kg/min)	Number of patients	Sensitivity	Specificity
Pennell, et al 1992 [88]	20	25	91	—
van Rugge, et al 1993 [66,90]	20	45	81	100
van Rugge, et al 1994 [91]	20	39	91	80
Nagel, et al 1999 [92]	20	208	86	86
Baer, 1994 [89]	20	35	84	-
Nagel, 1999 [92]	40 + atropine	172	86	86
Hundley, et al 1999 [87]	40 + atropine	163	83	83
Wahl, 2004 [98]	40 + atropine	160	89	84
Summary		847	86	84

respectively, for identifying at least 50% of epicardial coronary arterial luminal narrowings with contrast coronary arteriography.

Detection of viability

CMR also has been used for identifying left ventricular myocardial segments that, because of myocardial stunning or hibernation, display abnormal wall motion at rest and will improve in contractility after coronary arterial revascularization procedures. Early studies examining viability compared CMR with other modalities including DSE and radioisotope studies. Development of tagging has enabled better quantitative assessment of LV wall thickening indicative of viability. Recently, there have been several studies looking at specific characteristics of the myocardium, including movement of individual layers, circumferential shortening, and wall thickening, all of which represent important determinants of potential recovery after revascularization.

After an MI, the transmural extent of necrosis and decrease in LV ejection fraction can vary considerably. Using CMR tagging to regionally quantify fiber strains, wall thickening, and ejection fraction, Bogaert and colleagues [100] assessed 12 patients who had single-vessel disease 1 week and 3 months after successful reperfusion of a first transmural anterior MI. Improved subepicardial fiber shortening at the 3-month mark was associated with an improved regional LV wall motion and global LV ejection fraction.

Geskin and colleagues [101] demonstrated that myocardial function recovery at 8 weeks after MI was predicted by an increase in circumferential shortening in resting dysfunctional segments during dobutamine infusion. In a group of 20 patients with first reperfused MI, they noted that midmyocardial response and subepicardial response to dobutamine were predictive of subsequent functional recovery, but improvement in subendocardial layers was not.

Using tissue tagging, Sayad and colleagues [102] demonstrated how low-dose dobutamine CMR analysis of LV thickening predicts future recovery of systolic thickening after revascularization of epicardial coronary arteries, supplying regions of hibernating and stunned myocardium (Fig. 9). In a group of 10 patients with segmental wall motion abnormalities at rest, they found that CMR had a sensitivity of 89%, a specificity of 93%, a negative predictive value of 82%, and a positive predictive value of 96% for recovery of segmental function after revascularization. Although not the focus of their study, the authors alluded to the excellent correlation between end–systolic wall thickness at peak dobutamine infusion and after revascularization.

Dendale and colleagues [103] evaluated the feasibility of stress CMR use for the detection of viability after acute MI. CMR images were analyzed for wall motion abnormalities during low-dosage dobutamine stimulation in 37 patients who had recent MI. The authors concluded that low-dosage dobutamine CMR is a safe and accurate predictor recovery of wall motion abnormalities after MI, but this study was limited by the lack of quantitative analysis of the CMR images.

In a quantitative analysis, Saito and colleagues [104] showed that CMR was as effective as DSE

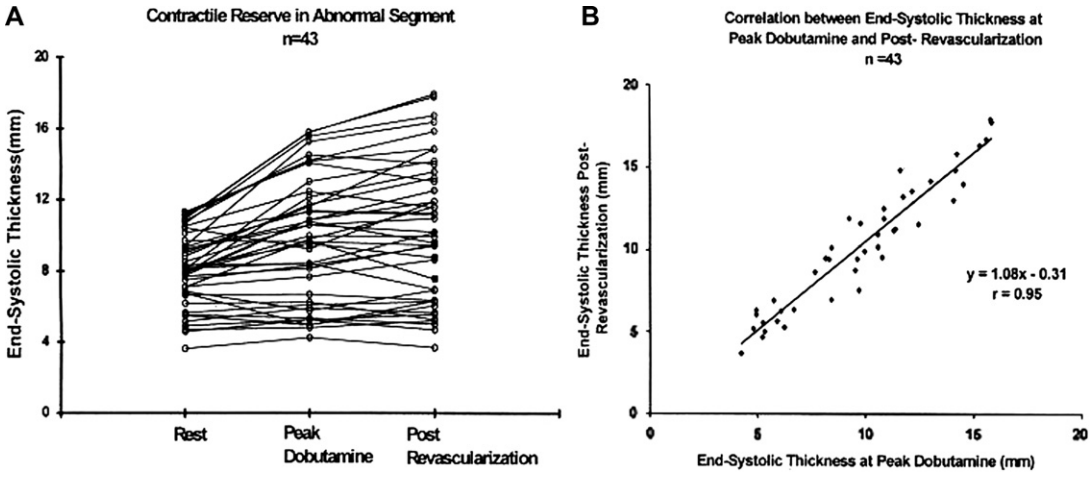

Fig. 9. Contractile reserve. (*A*) Plot of end–systolic wall thickening at rest, peak dobutamine, and after revascularization in all 43 abnormal segments. Squares represent the three segments that had contractile reserve with dobutamine, but no recovery of function after revascularization. Triangles represent the segment without contractile reserve, but this improved after revascularization. No segment with end–systolic wall thickness less than 7 mm had contractile reserve or improved after revascularization. (*B*) Regression line for end–systolic wall thickening at peak dobutamine and after revascularization. (*From* Sayad DE, Willett DL, Hundley WG, et al. Dobutamine magnetic resonance imaging with myocardial tagging quantitatively predicts improvement in regional function after revascularization. Am J Cardiol 1998;82(9):1149–51, A10; with permission.)

for identifying myocardial viability in subjects who had LV dysfunction at rest. Dobutamine CMR and stress echo had similar results in 86% of the patients for detecting myocardial viability. Sensitivity (76%) and specificity (86%) with CMR compared well with the sensitivity (66%) and specificity for DSE (100%). The sensitivity of DCMR with tagging was noted to be 76%, whereas that of DSE was 66%. The specificity of DCMR was 86%, and that of DSE was 100%. The accuracy of DCMR was 78%; that of DSE was 72%.

Dobutamine CMR has been compared with metabolic assessment of viability obtained during radionuclide studies. Baer and colleagues [89] reported that implementation of dobutamine stress provided further information regarding viability than resting LV end–diastolic wall thickness. End–diastolic wall thickness at rest and dobutamine-induced systolic wall thickening assessed by DCMR were compared with positron emission tomography (PET). They concluded that DCMR was a better predictor of residual metabolic activity, with sensitivity of 81%, specificity of 95%, and positive predictive accuracy of 96%, than PET, with a sensitivity of 72%. specificity of 89%, and positive predictive accuracy of 91%.

Delayed hyperenhancement techniques also have been used to identify myocardial necrosis and an absence of myocellular viability. In several small studies of 10 to 30 subjects, delayed enhancement imaging has been compared with dobutamine wall motion analyses for predicting the return of LV systolic function after coronary arterial revascularization [105–108]. In the most widely referenced of these studies, Wellnhofer and colleagues [108] compared recovery of systolic thickening as measured by CMR with delayed-enhancement imaging in 29 patients. Increased thickening during dobutamine CMR was more likely than delayed enhancement to identify improvement in contractility after revascularization in myocardial segments with the transmural extent of infarction less than 50%. For those with no or extensive infarcts, the techniques had similar efficacy.

Prognosis

Assessments of LV wall motion and ejection fraction can be used to predict long-term prognosis. In 2002, Hundley and colleagues [110] reported on the utility of dobutamine CMR for

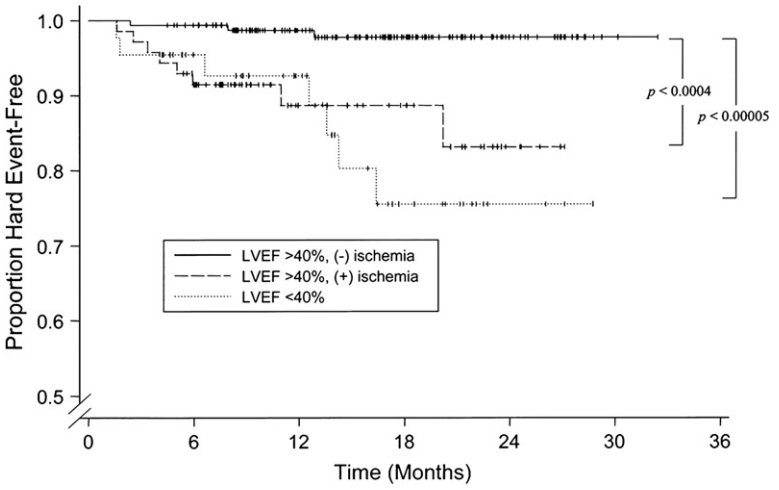

Fig. 10. Cardiovascular magnetic resonance prognosis. Kaplan-Meier event-free survival curves in patients who had an left ventricular ejection fraction (LVEF) less than 40% and greater than 40% with and without inducible ischemia. In patients who had an LVEF greater than 40%, the event-free survival was significantly lower in patients who had inducible ischemia compared with those who did not ($P < .0004$). An even greater difference was found between patients with patients who had an LVEF with 40% evidence of inducible ischemia compared with those with an LVEF less than 40% ($P < .00005$). (*From* Hundley WG, Morgan TM, Neagle CM, et al. Magnetic resonance imaging determination of cardiac prognosis. Circulation 2002;106(18):2328–33; with permission.)

identifying future myocardial infarction and cardiac death in 279 patients who were followed over an average of 20 months. In a multivariate analysis, inducible ischemia, contractile reserve, or low LV ejection fraction were associated with cardiac death and future MI, independent of the presence of risk factors for coronary arteriosclerosis or MI (Fig. 10).

CMR also has been used to determine preoperative cardiovascular risk in patients referred for noncardiac surgery. Rerkpattanapipat and colleagues [111] followed a group of 102 consecutive patients for the occurrence of cardiac death, MI, or congestive heart failure during or after noncardiac surgery. Six patients experienced a cardiac event (death in four, nonfatal myocardial

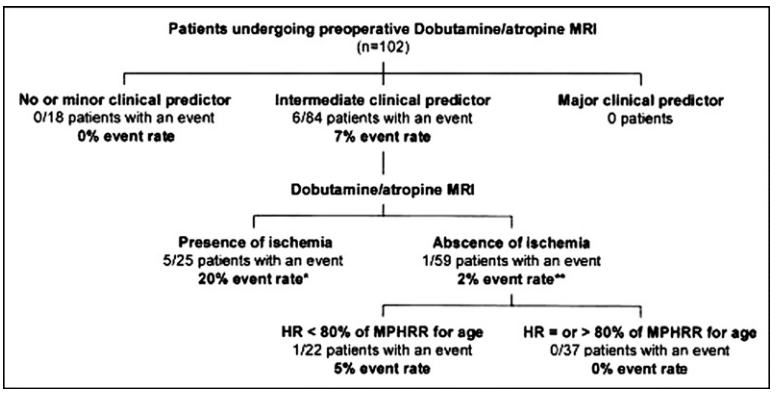

Fig. 11. Preoperative evaluation with cardiovascular magnetic resonance. The number of events and event rates for participants in the authors' study. As shown, those with inducible ischemia during dobutamine magnetic resonance imaging had a significant increase in the incidence of cardiac events. *Abbreviations:* HR, heart rate; MPHRR, maximal predicted heart rate response. (*From* Rerkpattanapipat P, Morgan TM, Neagle CM, et al. Assessment of preoperative cardiac risk with magnetic resonance imaging. Am J Cardiol 2002;90(4):416–9; with permission.)

Fig. 12. Exercise cardiovascular magnetic resonance (CMR). Diagrammatic representation of an exercise bike used for CMR stress studies made from nonferromagnetic materials (left panel). In the right panel, a treadmill positioned outside of the magnetic resonance scanner. With this treadmill approach, heightened diagnostic accuracy is achieved when images are collected within a minute of exercise cessation.

infarction in one, and congestive heart failure in one) during surgery or in their postoperative course. Five of 26 patients who had evidence of inducible ischemia during DCMR underwent revascularization before surgery (one sustained an event, and four did not). In patients who had intermediate clinical predictors of events as defined by the American College of Cardiology and the American Heart Association, evidence of inducible ischemia during CMR imaging was associated with a significant increase in perioperative cardiac events (Fig. 11).

Exercise stress testing

As with echocardiography, it may be possible to implement exercise instead of pharmacologic stress to obtain imaging. Studies have been conducted looking at both the bicycle and treadmill exercise as stress agents. Bicycle exercise has the advantage of reduction in stress protocol duration and acquisition of data regarding functional capacity. In one study, Roest and colleagues [112] studied 16 healthy volunteers (eight women and eight men, mean age 18 ± 2 years) with bicycle exercise in the supine position on a MR-compatible bicycle ergometer at 1.5 T. By breath holding at end expiration, image blurring was avoided because of respiratory motion for all short-axis images. Stroke volume and ejection fraction increased in both ventricles in response to exercise; as would be expected, the end–systolic volume of the two ventricles decreased, while the end–diastolic volumes remained the same This study demonstrates that exercise CMR, in normal patients, can be used to assess physiologic changes in both the left and right ventricles simultaneously (Fig. 12).

Although the previous study used supine bicycle exercise, Rerkpattanapipat and colleagues [109] used upright treadmill in 27 patients who had images obtained less than 1 minute after exercise (see Fig. 12). Ischemia was appreciated in 14 patients, with good overall sensitivity and specificity of detecting epicardial artery luminal narrowings greater than 50% of 79% and 85%, respectively. This study was limited, however, in that comprehensive coverage of the myocardium was not achieved, and results were acquired on a small number of subjects. Further studies are needed in this area to determine the clinical utility of exercise-induced wall motion abnormalities for the assessment of patients who have cardiovascular disease.

Summary

Several imaging techniques are available for assessing global and regional LV and RV function during cardiovascular MRI examinations. These techniques can be used to provide accurate and reproducible measures of ventricular volumes and ejection fraction. In those who can undergo CMR, it may be the most accurate noninvasive imaging test for determining LV or RV volumes or ejection fraction.

CMR also can be used to provide information about regional LV function including: wall motion, thickening, and strain. To date, these regional function measures have been acquired at rest and with stress, and they have been shown to be useful for identifying myocardial ischemia, injury, and viability. In addition, changes in regional function observed during dobutamine stress CMR are useful for assessing cardiac prognosis and preoperative cardiac risk assessment for noncardiac surgery.

References

[1] Haase A, Frahm J, Mathaei D. Rapid three-dimensional MR imaging using the FLASH technique J Comput Assist Tomogr 1986;67:256–66.

[2] Balaban R. The physics of image generation by magnetic resonance. In: Manning WJ, Pennell DJ, editors. Cardiovascular magnetic resonance. 1st edition. Philadelphia: Churchill Livingstone; 2002. p. 3–17.

[3] Mirowitz S, Eilenberg S, White R. Cardiac MR imaging techniques and strategies. In: Gutierrez F, Brown J, Mirowitz S, editors. Cardiovascular magnetic resonance imaging. Chicago: Mosby; 1992. p. 17–22.

[4] Masood S, Yang GZ, Pennell DJ, et al. Investigating intrinsic myocardial mechanics: the role of MR tagging, velocity phase mapping, and diffusion imaging. J Magn Reson Imaging 2000;12:873–83.

[5] Longmore DB, Klipstein RH, Underwood SR, et al. Dimensional accuracy of magnetic resonance in studies of the heart. Lancet 1985;1(8442):1360–2.

[6] Semelka RC, Tomei E, Wagner S, et al. Normal left ventricular dimensions and function: interstudy reproducibility of measurements with cine MR imaging. Radiology 1990;174(3 Pt 1):763–8.

[7] Debatin JF, Nadel SN, Paolini JF, et al. Cardiac ejection fraction: phantom study comparing cine MR imaging, radionuclide blood pool imaging, and ventriculography. J Magn Reson Imaging 1992;2(2):135–42.

[8] Germain P, Roul G, Kastler B, et al. Interstudy variability in left ventricular mass measurement. Comparison between M-mode echography and MRI. Eur Heart J 1992;13(8):1011–9.

[9] Sandstede J, Lipke C, Beer M, et al. Age- and gender-specific differences in left and right ventricular cardiac function and mass determined by cine magnetic resonance imaging. Eur Radiol 2000;10(3): 438–42.

[10] Salehian O, Schwerzmann M, Merchant N, et al. Assessment of systemic right ventricular function in patients with transposition of the great arteries using the myocardial performance index: comparison with cardiac magnetic resonance imaging. Circulation 2004;110(20):3229–33.

[11] Nitz W. Fast and ultrafast nonecho–planar MR imaging techniques. Eur Radiol 2002;12(12): 2866–82.

[12] Oppelt A, Graumann R, Barfuss A, et al. FISP: a new fast MRI sequence. Electromedica 1986;3: 15–8.

[13] Zur Y, Wood ML, Neuringer LJ. Motion-insensitive, steady-state free precession imaging. Magn Reson Med 1990;16:444–59.

[14] Duerk JL, Lewin JS, Wendt M, et al. Remember true FISP? A high SNR, near 1-second imaging method for T2-like contrast in interventional MRI at .2 T. J Magn Reson Imaging 1998;8:203–8.

[15] Chung YC, Merkle EM, Lewin JS, et al. Fast T(2)-weighted imaging by PSIF at 0.2 T for interventional MRI. Magn Reson Med 1999;42:335–44.

[16] Wendt M, Wacker F, Wolf KJ, et al. [Keyhole-true FISP: fast T2-weighted imaging for interventional MRT at 0.2 T]. Rofo 1999;170:391–3 [in German].

[17] Barkhausen J, Ruehm SG, Goyen M, et al. MR evaluation of ventricular function: true fast imaging with steady-state precession versus fast low-angle shot cine MR imaging: feasibility studyRadiology 2001;219:264–9.

[18] Fischer H, Ladebeck R. Echo-planar imaging image artifacts. In: Schmitt F, Stehling MK, Turner R, editors. Echo-planar imaging: theory, technique, and application. New York: Springer; 1998. p. 179–210.

[19] Weiger M, Pruessmann KP, Boesiger P. Cardiac real-time imaging using SENSE: sensitivity-encoding scheme. Magn Reson Med 2000;43:177–84.

[20] Pruessmann KP, Weiger M, Bornert P, et al. Advances in sensitivity encoding with arbitrary k-space trajectories. Magn Reson Med 2001;46: 638–51.

[21] Weiger M, Pruessmann KP, Leussler C, et al. Specific coil design for SENSE: a six-element cardiac array. Magn Reson Med 2001;45:495–504.

[22] Pruessmann KP, Weiger M, Boesiger P. Sensitivity-encoded cardiac MRI. J Cardiovasc Magn Reson 2001;3:1–9.

[23] Huang J, Abendschein D, Davila-Roman VG, et al. Spatio–temporal tracking of myocardial deformations with a 4-D B-spline model from tagged MRI. IEEE Trans Med Imaging 1999;18:957–72.

[24] Fischer SE, McKinnon GC, Maier SE, et al. Improved myocardial tagging contrast. Magn Reson Med 1993;30:191–200.

[25] Fischer SE, Stuber M, Dam J, et al. Late diastolic tag persistence with slice followed echo planar imaging. In: Proceedings of the 4th Scientific Meeting, New York: International Society of Magnetic Resonance 1; 1996:297.

[26] Aletras AH, Wen H. Mixed echo train acquisition displacement encoding with stimulated echoes: an optimized DENSE method for in vivo functional imaging of the human heart. Magn Reson Med 2001;46:523–34.

[27] Kim D, Gilson WD, Kramer CM, et al. Myocardial tissue tracking with two-dimensional cine displacement-encoded MR imaging: development and initial evaluation. Radiology 2004;230(3): 862–71.
[28] Rumancik W, Naidich D, Chandra R, et al. Cardiovascular disease: evaluation with MR phase imaging. Radiology 1988;166:63–8.
[29] Pelc LR, Sayre J, Yun K, et al. Evaluation of myocardial motion tracking with cine-phase contrast magnetic resonance imaging. Invest Radiol 1994; 29:1038–42.
[30] Jung B, Zaitsev M, Hennig J, et al. Navigator gated high temporal resolution tissue phase mapping of myocardial motion. Magn Reson Med 2006;55: 937–42.
[31] Markl M, Schneider B, Hennig J. Fast phase contrast cardiac magnetic resonance imaging: improved assessment and analysis of left ventricular wall motion. J Magn Reson Imaging 2002;15: 642–53.
[32] Jung B, Foll D, Bottler P, et al. Detailed analysis of myocardial motion in volunteers and patients using high temporal resolution MR tissue phase mapping. J Magn Reson Imaging 2006;24:1033–9.
[33] van Dijk P. Direct cardiac NMR imaging of heart wall and blood flow velocity. J Comput Assist Tomogr 1984;8:429–36.
[34] Wedeen VJ. Magnetic resonance imaging of myocardial kinematics. Technique to detect, localize, and quantify the strain rates of the active human myocardium. Magn Reson Med 1992;27:52–67.
[35] Nayler GL, Firmin DN, Longmore DB. Blood flow imaging by cine magnetic resonance. J Comput Assist Tomogr 1986;10:715–22.
[36] Petersen SE, Jung BA, Wiesmann F, et al. Myocardial tissue phase mapping with cine phase–contrast MR imaging: regional wall motion analysis in healthy volunteers. Radiology 2006;238:816–26.
[37] Van der Geest RJ, Reiber JH. Quantification in cardiac, MRI. J Magn Reson Imaging 1999;10: 602–8.
[38] Wedeen VJ, Weisskoff RM, Reese TG, et al. Motionless movies of myocardial strain—rates using stimulated echoes. Magn Reson Med 1995;33: 401–8.
[39] Rehr RB, Malloy CR, Filipchuk NG, et al. Left ventricular volumes measured by MR imaging-Radiology 1985;156:717–9.
[40] Chuang ML, Hibberd MG, Salton CJ, et al. Importance of imaging method over imaging modality in noninvasive determination of left ventricular volumes and ejection fraction: assessment by two- and three-dimensional echocardiography and magnetic resonance imaging. J Am Coll Cardiol 2000;35:477–84.
[41] Cranney GB, Lotan CS, Dean L, et al. Left ventricular volume measurement using cardiac axis nuclear magnetic resonance imaging. Validation by calibrated ventricular angiography. Circulation 1990;82:154–63.
[42] Lawson MA, Blackwell GG, Davis ND, et al. Accuracy of biplane long-axis left ventricular volume determined by cine magnetic resonance imaging in patients with regional and global dysfunction. Am J Cardiol 1996;77:1098–104.
[43] Martin ET, Fuisz AR, Pohost GM. Imaging cardiac structure and pump function. Cardiol Clin 1998;16:135–60.
[44] Keller AM, Peshock RM, Malloy CR, et al. In vivo measurement of myocardial mass using nuclear magnetic resonance imaging. J Am Coll Cardiol 1986;8(1):113–7.
[45] Koch JA, Poll LW, Godehardt E, et al. Right and left ventricular volume measurements in an animal heart model in vitro: first experiences with cardiac MRI at 1.0 T. Eur Radiol 2000;10(3): 455–8.
[46] Nahrendorf M, Hiller KH, Hu K, et al. Cardiac magnetic resonance imaging in small animal models of human heart failure. Med Image Anal 2003;7(3):369–75.
[47] Caputo G, Tscholakoff D, Sechtem U, et al. Measurement of canine left ventricular mass by using MR imaging. AJR Am J Roentgenol 1987;148: 33–8.
[48] Holman ER, Vliegen HW, van der Geest RJ, et al. Quantitative analysis of regional left ventricular function after myocardial infarction in the pig assessed with cine magnetic resonance imaging. Magn Reson Med 1995;34:161–9.
[49] Rudin M, Pedersen B, Umemura K, et al. Determination of rat heart morphology and function in vivo in two models of cardiac hypertrophy by means of magnetic resonance imaging. Basic Res Cardiol 1991;86(2):165–74.
[50] Pattynama PM, Lamb HJ, van der Velde EA, et al. Left ventricular measurements with cine and spin echo MR imaging: a study of reproducibility with variance component analysis. Radiology 1993; 187:261–8.
[51] Semelka RC, Tomei E, Wagner S, et al. Interstudy reproducibility of dimensional and functional measurements between cine magnetic resonance studies in the morphologically abnormal left ventricle. Am Heart J 1990;119:1367–73.
[52] Stratemeier EJ, Thompson R, Brady TJ, et al. Ejection fraction determination by MR imaging: comparison with left ventricular angiography. Radiology 1986;158:775–7.
[53] Shapiro EP, Rogers WJ, Beyar R, et al. Determination of left ventricular mass by MRI in hearts deformed by acute infarction. Circulation 1989;79: 706–11.
[54] Meyer S, Curry G, Donsky M, et al. Influence of dobutamine on hemodynamics and coronary blood flow in patients with and without coronary artery disease. Am J Cardiol 1976;38:103–8.

[55] Lee VS, Resnick D, Bundy JM, et al. Cardiac function: MR evaluation in one breath hold with real-time true fast imaging with steady-state precession. Radiology 2002;222:835–42.
[56] Boxt LM, Katz J. Magnetic resonance imaging for quantitation of right ventricular volume in patients with pulmonary hypertension. J Thorac Imaging 1993;8:92–7.
[57] Doherty NE III, Fujita N, Caputo GR, et al. Measurement of right ventricular mass in normal and dilated cardiomyopathic ventricles using cine magnetic resonance imaging. Am J Cardiol 1992;69: 1223–8.
[58] Katz J, Whang J, Boxt LM, et al. Estimation of right ventricular mass in normal subjects and in patients with primary pulmonary hypertension by nuclear magnetic resonance imaging. J Am Coll Cardiol 1993;21:1475–81.
[59] Pattynama PM, Lamb HJ, van der Velde EA, et al. Reproducibility of MRI-derived measurements of right ventricular volumes and myocardial mass. Magn Reson Imaging 1995;13:53–63.
[60] Rominger MB, Bachmann GF, Pabst W, et al. Right ventricular volumes and ejection fraction with fast cine MR imaging in breath-hold technique: applicability, normal values from 52 volunteers, and evaluation of 325 adult cardiac patients. J Magn Reson Imaging 1999;10:908–18.
[61] Lorenz CH, Walker ES, Morgan VL, et al. Normal human right and left ventricular mass, systolic function, and gender differences by cine magnetic resonance imaging. J Cardiovasc Magn Reson 1999;1:7–21.
[62] Azhari H, Sideman S, Weiss JL, et al. Three-dimensional mapping of acute ischemic regions using MRI: wall thickening versus motion analysis. Am J Physiol 1990;259:1492–503.
[63] Henschke CI, Risser TA, Sandor T, et al. Quantitative computer-assisted analysis of left ventricular wall thickening and motion by two-dimensional echocardiography in acute myocardial infarction. Am J Cardiol 1983;52:960–4.
[64] Lieberman AN, Weiss JL, Jugdutt BI, et al. Two-dimensional echocardiography and infarct size: relationship of regional wall motion and thickening to the extent of myocardial infarction in the dog. Circulation 1981;63:739–46.
[65] Holman ER, van Jonbergen HP, van Dijkman PR, et al. Comparison of magnetic resonance imaging studies with enzymatic indexes of myocardial necrosis for quantification of myocardial infarct size. Am J Cardiol 1993;71:1036–40.
[66] van Rugge FP, Holman ER, van der Wall EE, et al. Quantitation of global and regional left ventricular function by cine magnetic resonance imaging during dobutamine stress in normal human subjects. Eur Heart J 1993;14:456–63.
[67] Reichek N. MRI myocardial tagging. J Magn Reson Imaging 1999;10:609–16.
[68] Wang J, Urheim S, Korinek J, et al. Analysis of postsystolic myocardial thickening work in selective myocardial layers during progressive myocardial ischemia. J Am Soc Echocardiogr 2006;19(9): 1102–11.
[69] Edvardsen T, Rosen BD, Pan L, et al. Regional diastolic dysfunction in individuals with left ventricular hypertrophy measured by tagged magnetic resonance imaging—the Multi-Ethnic Study of Atherosclerosis (MESA). Am Heart J 2006; 151(1):109–14.
[70] Lima JA, Jeremy R, Guier W, et al. Accurate systolic wall thickening by nuclear magnetic resonance imaging with tissue tagging: correlation with sonomicrometers in normal and ischemic myocardium. J Am Coll Cardiol 1993;21:1741–51.
[71] Yeon SB, Reichek N, Tallant BA, et al. Validation of in vivo myocardial strain measurement by magnetic resonance tagging with sonomicrometry J Am Coll Cardiol 2001;38:555–61.
[72] Fonseca CG, Dissanayake AM, Doughty RN, et al. Three-dimensional assessment of left ventricular systolic strain in patients with type 2 diabetes mellitus, diastolic dysfunction, and normal ejection fraction. Am J Cardiol 2004;94(11):1391–5.
[73] Palmon LC, Reichek N, Yeon SB, et al. Intramural myocardial shortening in hypertensive left ventricular hypertrophy with normal pump function. Circulation 1994;89:122–31.
[74] Bogaert J, Bosmans H, Maes A, et al. Remote myocardial dysfunction after acute anterior myocardial infarction: impact of left ventricular shape on regional function: a magnetic resonance myocardial tagging study. J Am Coll Cardiol 2000;35:1525–34.
[75] Marcus JT, Gotte MJ, Van Rossum AC, et al. Myocardial function in infarcted and remote regions early after infarction in man: assessment by magnetic resonance tagging and strain analysis. Magn Reson Med 1997;38:803–10.
[76] Paetsch I, Foll D, Kaluza A, et al. Magnetic resonance stress tagging inischemic heart disease. Am J Physiol Heart Circ Physiol 2005;288:H2708–14.
[77] Rebergen SA, Ottenkamp J, Doornbos J, et al. Postoperative pulmonary flow dynamics after Fontan surgery: assessment with nuclear magnetic resonance velocity mapping. J Am Coll Cardiol 1993;21:123–31.
[78] Holmqvist C, Oskarsson G, Stahlberg F, et al. Functional evaluation of extracardiac ventriculopulmonary conduits and of the right ventricle with magnetic resonance imaging and velocity mapping. Am J Cardiol 1999;83:926–32.
[79] Fogel MA. Assessment of cardiac function by magnetic resonance imaging. Pediatr Cardiol 2000;21: 59–69.
[80] Saito H, Dambara T, Aiba M, et al. Evaluation of cor pulmonale on a modified short-axis section of the heart by magnetic resonance imaging. Am Rev Respir Dis 1992;146:1576–81.

[81] Pattynama PM, Willems LN, Smit AH, et al. Early diagnosis of cor pulmonale with MR imaging of the right ventricle. Radiology 1992;182:375–9.
[82] Boxt LM. MR imaging of pulmonary hypertension and right ventricular dysfunction. Magn Reson Imaging Clin N Am 1996;4:307–25.
[83] Casolo GC, Poggesi L, Boddi M, et al. ECG-gated magnetic resonance imaging in right ventricular dysplasia. Am Heart J 1987;113:1245–8.
[84] Blake LM, Scheinman MM, Higgins CB. MR features of arrhythmogenic right ventricular dysplasia. Am J Roentgenol 1994;162:809–12.
[85] McKenna WJ, Thiene G, Nava A, et al. Diagnosis of arrhythmogenic right ventricular dysplasia/cardiomyopathy. Task Force of the Working Group Myocardial and Pericardial Disease of the European Society of Cardiology and of the Scientific Council on Cardiomyopathies of the International Society and Federation of Cardiology. Br Heart J 1994;71:215–8.
[86] Keller D, Osswald S, Bremerich J, et al. Arrhythmogenic right ventricular dysplasia: diagnostic and prognostic value of cardiac MRI in relation to arrhythmia-free survival. Int J Card Imaging 2003;19:537–43.
[87] Hundley WG, Hamilton CA, Thomas MS, et al. Utility of fast cine magnetic resonance imaging and display for the detection of myocardial ischemia in patients not well-suited for second harmonic stress echocardiography. Circulation 1999;100:1697–702.
[88] Pennell DJ, Underwood SR, Manzara CC, et al. Magnetic resonance imaging during dobutamine stress in coronary artery disease. Am J Cardiol 1992;70(1):34–40.
[89] Baer FM, Theissen P, Smolarz K, et al. Dobutamine versus dipyridamole magnetic resonance tomography: safety and sensitivity in the detection of coronary stenosis. Z Kardiol 1993;82:494–503.
[90] van Rugge FP, van der Wall EE, de Roos A, et al. Dobutamine stress magnetic resonance imaging for detection of coronary artery disease. J Am Coll Cardiol 1993;22:431–9.
[91] van Rugge FP, van der Wall EE, Spanjersberg SJ, et al. Magnetic resonance imaging during dobutamine stress for detection and localization of coronary artery disease. Quantitative wall motion analysis using a modification of the centerline method. Circulation 1994;90:127–38.
[92] Nagel E, Lehmkuhl HB, Bocksch W, et al. Noninvasive diagnosis of ischemia-induced wall motion abnormalities with the use of high-dose dobutamine stress magnetic resonance imaging: comparison with dobutamine stress echocardiography. Circulation 1999;99:763–70.
[93] Wahl A, Roethemeyer S, Paetsch I, et al. High-dose dobutamine stress MRI for follow-up after coronary revascularization procedures in patients with wall motion abnormalities at rest. J Cardiovasc Magn Reson 2002;4:22–3.
[94] Wahl A, Roethemeyer S, Paetsch I, et al. Simultaneous assessment of wall motion and myocardial perfusion during high-dose dobutamine stress MRI improves diagnosis of ischemia in patients with known coronary artery disease. J Cardiovasc Magn Reson 2002;4:136–7.
[95] Sensky PR, Jivan A, Hudson N, et al. Coronary artery disease: combined stress MR imaging protocol—one-stop evaluation of myocardial perfusion and function. Radiology 2000;215:608–14.
[96] Paetsch I, Jahnke C, Wahl A, et al. Comparison of dobutamine stress magnetic resonance, adenosine stress magnetic resonance, and adenosine stress magnetic resonance perfusion. Circulation 2004; 110:835–42.
[97] Zoghbi WA, Barasch E, Dobutamine MRI. A serious contender in pharmacological stress imaging? Circulation 1999;99(6):730–2.
[98] Wahl A, Paetsch I, Roethemeyer S, et al. High-dose dobutamine–atropine stress cardiovascular MR imaging after coronary revascularization in patients with wall motion abnormalities at rest. Radiology 2004;233:210–6.
[99] Kuijpers D, Ho KY, van Dijkman PR, et al. Dobutamine cardiovascular magnetic resonance for the detection of myocardial ischemia with the use of myocardial tagging. Circulation 2003; 107(12):1592–7.
[100] Bogaert J, Maes A, Rademakers FE. Functional recovery of subepicardial myocardial tissue in transmural myocardial infarction after successful reperfusion: an important contribution to the improvement of regional and global left ventricular function. Circulation 1999;99(1):36–43.
[101] Geskin G, Kramer CM, Rogers WJ, et al. Quantitative assessment of myocardial viability after infarction by dobutamine magnetic resonance tagging. Circulation 1998;98(3):217–23.
[102] Sayad DE, Willett DL, Hundley WG, et al. Dobutamine magnetic resonance imaging with myocardial tagging quantitatively predicts improvement in regional function after revascularization. Am J Cardiol 1998;82(9):1149–51, A10.
[103] Dendale PA, Franken PR, Waldman GJ, et al. Low-dosage dobutamine magnetic resonance imaging as an alternative to echocardiography in the detection of viable myocardium after acute infarction. Am Heart J 1995;130(1):134–40.
[104] Saito I, Watanabe S, Masuda Y. Detection of viable myocardium by dobutamine stress tagging magnetic resonance imaging with three-dimensional analysis by automatic trace method. Jpn Circ J 2000;64(7):487–94.
[105] Motoyasu M, Sakuma H, Ichikawa Y, et al. Prediction of regional functional recovery after acute myocardial infarction with low-dose dobutamine stress cine MR imaging and contrast-enhanced MR imaging. J Cardiovasc Magn Reson 2003; 5(4):563–74.

[106] Kaandorp TA, Bax JJ, Schuijf JD, et al. Head-to-head comparison between contrast-enhanced magnetic resonance imaging and dobutamine magnetic resonance imaging in men with ischemic cardiomyopathy. Am J Cardiol 2004;93(12): 1461–4.

[107] Rerkpattanapipat P, Little WC, Clark HP, et al. Effect of the transmural extent of myocardial scar on left ventricular systolic wall thickening during intravenous dobutamine administration. Am J Cardiol 2005;95(4):495–8.

[108] Wellnhofer E, Olariu A, Nagel E, et al. Magnetic resonance low-dose dobutamine test is superior to SCAR quantification for the prediction of functional recovery. Circulation 2004;109(18):2172–4.

[109] Rerkpattanapipat P, Darty SN, Hundley WG, et al. Feasibility to detect severe coronary artery stenoses with upright treadmill exercise magnetic resonance imaging. Am J Cardiol 2003;92(5):603–6.

[110] Hundley WG, Morgan TM, Neagle CM, et al. Magnetic resonance imaging determination of cardiac prognosis. Circulation 2002;106(18):2328–33.

[111] Rerkpattanapipat P, Morgan TM, Neagle CM, et al. Assessment of preoperative cardiac risk with magnetic resonance imaging. Am J Cardiol 2002; 90(4):416–9.

[112] Roest AA, Kunz P, Lamb HJ, et al. Biventricular response to supine physical exercise in young adults assessed with ultrafast magnetic resonance imaging. Am J Cardiol 2001;87:601–5.